



This is the accepted manuscript made available via CHORUS. The article has been published as:

Nonequilibrium interfacial diffusivity resolves anomalies in monolayer hydrodynamics

Tyler J. Mucci, Bruce L. Liu, Joe A. Adam, Amir H. Hirsa, Jason Yalim, and Juan M. Lopez

Phys. Rev. E **111**, L013501 — Published 2 January 2025

DOI: 10.1103/PhysRevE.111.L013501

Non-equilibrium interfacial diffusivity resolves anomalies in monolayer hydrodynamics

Tyler J. Mucci, Bruce L. Liu, Joe A. Adam, and Amir H. Hirsa
Department of Mechanical, Aerospace and Nuclear Engineering, Rensselaer Polytechnic Institute, Troy, New York 12180, USA

Jason Yalim and Juan M. Lopez
School of Mathematical and Statistical Sciences, Arizona State University, Tempe, Arizona 85287, USA

(Dated: November 18, 2024)

Hydrodynamics of surfactant monolayers are governed by surface tension, surface shear viscosity, surface dilatational viscosity and surface diffusivity. While the first two have been studied comprehensively with consistent results, surface dilatational viscosity is plagued with anomalies, including apparent negative values. Here, full-field interfacial velocity measurements together with the Navier–Stokes equations reveal that a source of these anomalies is the use of equilibrium surface diffusivity for systems far from equilibrium. Specifically, surface diffisivity was found to be more than 7 orders of magnitude (10 million times) larger in a non-solenoidal interfacial flow field. Micron-sized phase domains in the monolayer are the likely culprit for the enhanced diffusivity.

Introduction.—Surfactant molecules are pervasive at air-water interfaces in nearly all natural and man-made systems [1]. The defining tendency of surfactant molecules is to collect in a monomolecular layer at the interface, reducing surface tension [2]. Consequently, monotonic decreases in surface tension with increasing surfactant monolayer concentration impart elasticity to the interface [3, 4]. Monolayer-covered interfaces in flowing systems remain a challenge to model due to flow-induced non-uniformity in concentration, even when the interface is flat. Aside from surface elasticity, surfactant monolayers exhibit interfacial (excess) viscosities, representing viscous resistance to both shear and compression/expansion [2, 3]. Equilibrium or near-equilibrium surface tension is straightforward to measure when the concentration is essentially uniform [2]. Furthermore, consistent measurements of surface shear viscosity have been obtained in various flow geometries and flow regimes for both Newtonian and non-Newtonian monolayers, again when the monolayer concentration is essentially uniform [3, 5, 6]. On the other hand, surface dilatational viscosity has proven much more perplexing. For a given surfactant, variations on the order of 10^5 between different measurement techniques have been reported [3] as well as other anomalies including non-physical negative values [7–9]. For soluble surfactants, there is some understanding of why the measurement techniques lead to negative values [10], having to do with adsorption and desorption time scales and the frequencies at which the interface is compressed and expanded, but for insoluble surfactants the issue remains. This state of affairs arises because in order for surface dilatational viscosity effects to manifest, the monolayer concentration needs to be driven away from uniformity (equilibrium). Surface dilatational viscosity, surface elasticity and surface diffusivity act in unison, making their distinction challenging [11]. This Letter shows that a fundamental issue for systems far from equilibrium, where surface dilatational viscosity manifests, is equilibrium binary diffusivity failing to be applicable.

The monolayer used in this study is 1,2-Dipalmitoylphosphatidylcholine (DPPC), the primary constituent of mammalian lung surfactant [12]. Aside from wide use in scientific studies, DPPC is insoluble in water, thus avoiding confounding issues with transport into the bulk fluid. Furthermore, to avoid interfacial stresses associated with interface creation and annihilation [13], bulk flow inertia is used to periodically compress and expand the monolayer while the interface remains flat and fixed in space using an oscillatory driven channel (see bottom panel of Fig. 1). It consists of two stationary sidewalls of height $H = 0.5\,\mathrm{cm}$ and horizontal distance $2H$ apart, with the floor harmonically oscillating horizontally at angular frequency ω with displacement amplitude δ and corresponding maximal speed $U = \delta\omega$ [14]. The channel is filled to the brim with water at 22 °C, kinematic viscosity $\nu = 9.57 \times 10^{-3}\mathrm{cm}^2/\mathrm{s}$ and dynamic viscosity $\mu = 9.55 \times 10^{-3}\mathrm{g}/(\mathrm{cm\ s})$. The span of the channel is $7H$, and for the flow regimes considered, the flow in the mid-span of the channel is essentially spanwise invariant allowing for a two-dimensional (2D) approximation [15]. The motion of the floor generates an alternating pair of vortices that drive a non-solenoidal velocity at the interface, resulting in periodic localized compressions and expansions of the monolayer. A snapshot from a numerical simulation of the flow is presented in Fig. 1 and the supplementary movie [16] animates the flow.

Theory.—The 2D flow is governed by the incompressible Navier–Stokes equations, non-dimensionalized using length scale H and time scale H/U,

$$\frac{\partial \boldsymbol{u}}{\partial t} + (\boldsymbol{u}\cdot\boldsymbol{\nabla})\boldsymbol{u} = -\boldsymbol{\nabla}p + \frac{1}{\mathrm{Re}}\boldsymbol{\nabla}^2\boldsymbol{u}, \quad \boldsymbol{\nabla}\cdot\boldsymbol{u} = 0, \tag{1}$$

where $\boldsymbol{u}(x,y,t) = (u(x,y,t), v(x,y,t))$ and $\mathrm{Re} = UH/\nu$ is the Reynolds number. The boundary conditions are no-slip on the vertical walls and oscillating floor: $u(\pm 1, y, t) = v(\pm 1, y, t) = 0$, $v(x, 0, t) = 0$ and $u(x, 0, t) = \sin(\Omega t)$, where $\Omega = \omega H/U$ is the non-dimensional frequency. The top surface is covered by an initially uniform monolayer of DPPC at concentration c_0 with corresponding surface tension σ_0^*. At the flat interface $y = 1$, the vertical velocity is $v = 0$, whereas

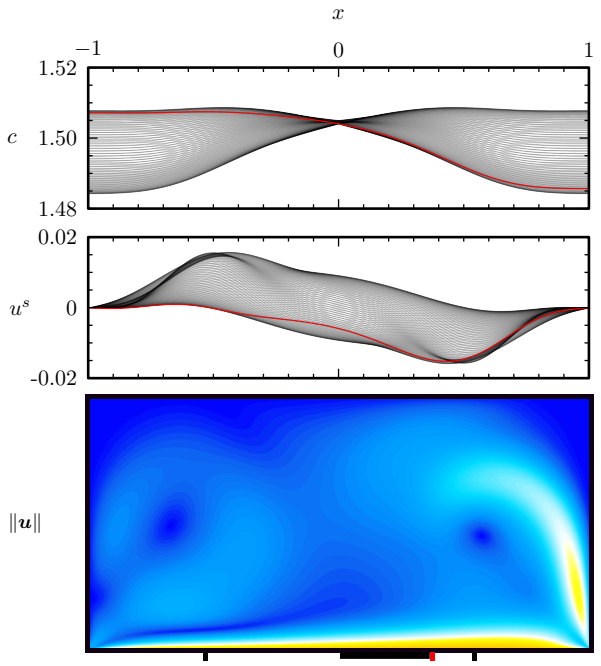


FIG. 1. Snapshot from a numerical simulation of the velocity magnitude $\|\boldsymbol{u}\|$ in the channel, together with profiles of surface velocity u^s and monolayer concentration c [17]. The supplemental movie [16] animates these over one floor oscillation. The black bar with red head at the bottom of the channel schematically indicates the instantaneous relative position of the oscillating floor. Flow parameters are: $\mathrm{Re} = 600$, $\Omega = 1/3$, $c_0 = 1.5\,\mathrm{mg/m^2}$, $\mathrm{Ca} = 1.645 \times 10^{-3}$, $\mathrm{Sc} = 0.0023$, and $\mathrm{Bq} = 1$.

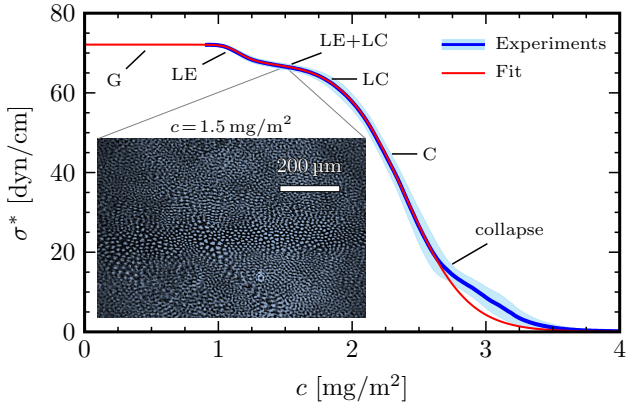


FIG. 2. Measured equation of state for DPPC at 22 °C and a curve fit $\sigma^*(c) = 67.31[1 + (c/2.63)^{9.06}]^{-1.889} + 4.80[1 + (c/1.13)^{22.14}]^{-0.578}$ dyn/cm. Labels indicate midpoints of monolayer phases [18]: gaseous G, liquid expanded LE, coexistent liquid expanded/condensed LE+LC, liquid condensed LC, condensed C, and point of collapse. The inset shows a Brewster angle microscopy (BAM) image of LE+LC domains [19].

the horizontal velocity at the surface, u^s, is determined by viscous coupling between the solenoidal bulk flow and the non-solenoidal interfacial flow using the Boussinesq–Scriven surface model for Newtonian gas-liquid interfaces [3, 13]. The coupling between the bulk and interfacial flows is given by the interfacial tangential stress balance

$$\left.\frac{\partial u}{\partial y}\right|_{y=1} = \frac{1}{\mathrm{Ca}}\frac{\partial \sigma}{\partial x} + \mathrm{Bq}\frac{\partial^2 u^s}{\partial x^2}, \tag{2}$$

where $\sigma = \sigma^*/\sigma_0^*$, $\mathrm{Ca} = \mu U/\sigma_0^*$ is the capillary number and $\mathrm{Bq} = (\kappa^s + \mu^s)/(\mu H)$ is the Boussinesq number, with surface shear viscosity μ^s and surface dilatational viscosity κ^s. This coupling results from balancing the bulk shear stress exerted at the interface with the surface tension gradients associated with surface elasticity and the contributions from surface viscosities [3].

The Boussineq–Scriven surface model is based on the premise that interfacial stress is due to gradients in the thermodynamic (equilibrium) surface tension and that any departures from equilibrium are accounted for by dissipation associated with the interfacial viscosities [13]. The Marangoni stress, the first term on the right-hand side of Eq. (2), requires the surface tension equation of state $\sigma^*(c)$ and the surfactant concentration distribution. Surface tension, being an equilibrium quantity, is measured quasi-statically by a slow compression in a Langmuir trough and a Wilhelmy plate tensiometer. Figure 2 presents our measured equation of state for DPPC and a curve fit used in the numerical simulations.

Transport of the surfactant concentration c is governed by the interfacial advection-diffusion equation

$$\frac{\partial c}{\partial t} + \frac{\partial}{\partial x}(c\,u^s) = \frac{1}{\mathrm{Re}\ \mathrm{Sc}}\frac{\partial^2 c}{\partial x^2}, \tag{3}$$

where $\mathrm{Sc} = \nu/D^s$ is the monolayer Schmidt number and D^s is the monolayer diffusivity. For systems at equilibrium, the diffusivity is $D^s \sim 10^{-7}\,\mathrm{cm^2/s}$ [11, 20]. However, co-existing phase domains of the monolayer can in principle undergo concerted motion, termed rafting [21], and act as nucleation sites for association and disassociation of surfactant molecules [22]. Both of these processes can significantly enhance mesoscale diffusion, leading to an interfacial diffusivity under dynamic conditions driving the interface out of equilibrium that is much larger than the interfacial diffusivity associated with systems at or near equilibrium [11].

Point velocity measurements have been previously used to study surface dilatational viscosity [3, 23, 24]. Point measurements do not allow deciphering effects of enhanced diffusivity. As such, distinguishing between multiple competing interfacial processes to produce unique combinations of properties is not possible. Here, full-field interfacial velocity measurements, along with numerical simulations, are used to interrogate the different interfacial transport processes for monolayers with gradients in concentration.

Methods.—Temporally and spatially resolved measurements of interfacial velocity u^s were performed across the full width of the channel (1 cm) at various Re and Ω for

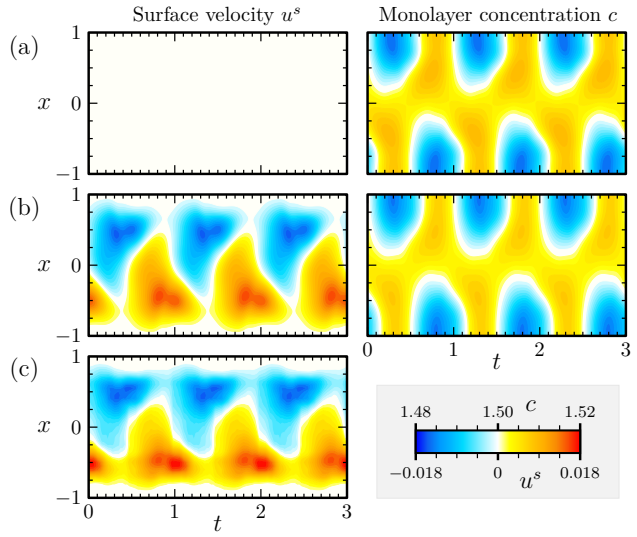


FIG. 3. Space-time plots of u^s and c from (a,b) two numerical simulations and (c) the laboratory experiment, for Re = 600, $\Omega = 1/3$, $c_0 = 1.5\,\mathrm{mg/m^2}$, and Ca $= 1.645 \times 10^{-3}$. In both numerical simulations Bq = 1, but Sc $= 10^5$ in (a) and Sc = 0.0023 in (b).

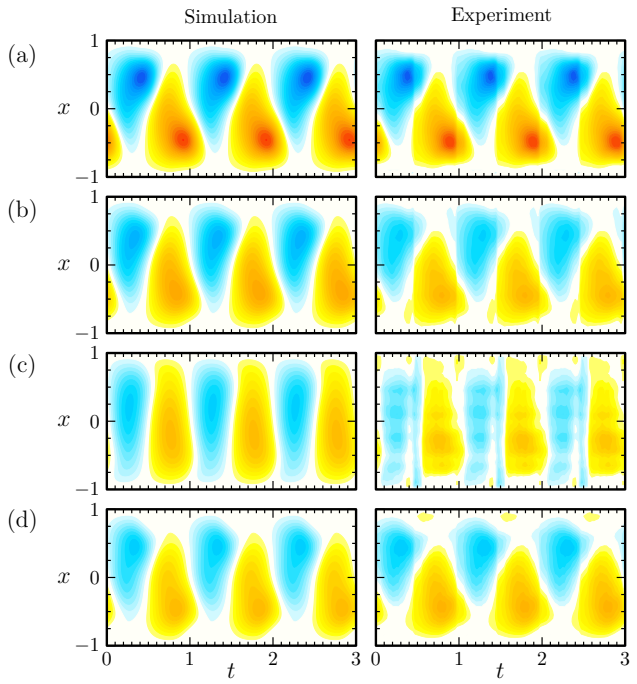


FIG. 4. Space-time plots of u^s from simulations and experiments at $c_0 = 1.5\,\mathrm{mg/m^2}$, Bq = 1, Sc = 0.0023 and various (Re, Ω): (a) $(200, 1/3)$, (b) $(200, 1/2)$, (c) $(200, 1)$, and (d) $(400, 1/2)$. For Re = 200 and 400, Ca $= 5.483 \times 10^{-4}$ and 8.225×10^{-4} respectively. Color-bar is same as in Fig. 3.

DPPC monolayers with $c_0 = 1.5\,\mathrm{mg/m^2}$ corresponding to the coexistent liquid expanded/condensed phases (see inset in Fig. 2 for a Brewster angle microscopy image of the monolayer). For all the experiments, the maximum variation in the surface concentration is less than 10% of c_0, avoiding issues associated with monolayer collapse occuring at $\sim 3\,\mathrm{mg/m^2}$, which may lead to the formation of micelles or vesicles in the bulk phase. Flatness of the interface was verified experimentally via a laser surface-slope probe. DPPC (Avanti Polar Lipids 850355C) was spread as a monolayer onto the interface using the standard technique of dissolution in a water-immiscible solvent (chloroform) [25]. Subsequently, the floor was oscillated for many periods before data acquisition to avoid flow transients and allow for solvent evaporation. After this initialization period, the surface was sparsely seeded with clean tracer particles of size $\sim 100\mu$m and imaged over multiple oscillations. Resulting image sequences underwent particle tracking velocimetry and phase averaging over all captured oscillations to produce u^s distributions over the width of the channel and one oscillation period. These measurements, further averaged over three replicates, were subsequently compared to numerical simulations to determine interfacial properties.

The numerical simulations were performed using a second-order finite-difference solver used in previous studies [9]. Multi-parameter sweeps in Sc and Bq were computed in order to minimize the root mean square error between measured and computed $u^s(x,t)$.

Results.—Figure 3 shows space-time plots of simulated $u^s(x,t)$ and $c(x,t)$ and experimental measurements of $u^s(x,t)$ over three floor oscillation periods for Re = 600, $\Omega = 1/3$ and a DPPC monolayer with $c_0 = 1.5\,\mathrm{mg/m^2}$. The simulation in Fig. 3(a) used Sc $= 10^5$, corresponding to equilibrium surface diffusivity $D^s \sim 10^{-7}$ cm^2/s, and Bq = 1. For any Bq between 0 and 100, simulations with Sc $= 10^5$ resulted in interfacial velocities orders of magnitude smaller than experimental measurements, without variation in u^s. On the other hand, keeping Bq = 1 but increasing surface diffusivity to $D^s \sim 4.2\,\mathrm{cm^2/s}$, corresponding to Sc = 0.0023, results in c slightly more diffused but a significantly larger u^s (Fig. 3b). With this high diffusivity the simulated u^s reproduces the experimental u^s very well (Fig. 3c). Note that the concentration distribution is not determined solely by diffusive effects, but also by the flow. The concentration and the flow are not only viscously coupled, but the whole system is nonlinear. While large differences in surface diffusivity only result is small differences in the concentration distribution, these lead to large differences in the surface velocity, to a large extent due to Marangoni stresses.

Figure 4 compares simulated and measured u^s for a number of different Re, Ω, and Ca, while holding Bq = 1 and Sc = 0.0023. The agreements are uniformly good over the range of Re $\in [200, 600]$ and $\Omega \in [1/3, 1]$.

Discussion.—Full-field measurements of $u^s(x,t)$ (Figs. 3 and 4) demonstrate that models of interfacial behavior using D^s obtained for monolayers in equilibrium do not predict interfacial velocity. Fitting to experimental data required D^s seven orders of magnitude larger than that for equilibrium systems. In

the context of a system forced far from equilibrium, co-existing phase domains provide a mechanism for a large enhancement of the interfacial diffusivity induced by non-solenoidal interfacial flow. Specifically, as suggested by previous monolayer diffusivity studies [22, 26], the square of the ratio between the macroscale (width of the oscillatory-driven channel $\sim 1\,\mathrm{cm}$) and the mesoscale of co-existing phase domains (between 1 and $10\,\mu\mathrm{m}$ for DPPC) provides the expected seven orders of magnitude increase in interfacial diffusivity compared to equilibrium binary diffusivity.

These results provide, perhaps for the first time, a consistent realization of the Boussinesq–Scriven surface model applied to a monolayer under periodic compression and expansion that results in monolayer concentration gradients. The parameter regime considered (scale of the channel, along with the frequency and amplitude of the floor oscillation) was sufficient to establish that the Boussinesq number Bq (non-dimensional sum of the surface viscosities) is indeed positive when surface diffusivity is taken to be much larger than the generally used equilibrium value. Using the equilibrium surface diffusivity within the Boussinesq–Scriven surface model results in negative Bq being needed to obtain surface velocities of the same magnitude as in experiments. A possible explanation is that the co-exisiting liquid expanded and liquid condensed domains of the monolayer phase act as pockets of condensed matter resulting in the larger non-equilibrium surface diffusivity. This resolves a long-standing issue where the surface viscosity was misinterpreted to be negative.

Acknowledgments.—The authors thank Jerry Z. Huang for assistance in constructing the experimental apparatus and Patrick Underhill for comments and feedback on the modeling of interfacial viscosity. This work was supported by US National Science Foundation grants 2204081, 2204082 and 2323020.

[1] J. C. Scott, The preparation of water for surface-clean fluid mechanics, J. Fluid Mech. **69**, 339 (1975).
[2] A. Adamson and A. Gast, *Physical Chemistry of Surfaces* (Wiley, 1997).
[3] D. Edwards, H. Brenner, and D. Wasan, *Interfacial Transport Processes & Rheology* (Butterworths, 1991).
[4] J. C. Slattery, L. M. C. Sagis, and E.-S. Oh, *Interfacial Transport Phenomena*, 2nd ed. (Springer, 2007).
[5] A. Sadoughi, J. M. Lopez, and A. H. Hirsa, Transition from Newtonian to non-Newtonian surface shear viscosity of phospholipid monolayers, Phys. Fluids **25**, 032107 (2013).
[6] A. Raghunandan, A. H. Hirsa, P. T. Underhill, and J. M. Lopez, Predicting steady shear rheology of condensed-phase monomolecular films at the air-water interface, Phys. Rev. Lett. **121**, 164502 (2018).
[7] J. Giermanska-Kahn, F. Monroy, and D. Langevin, Negative effective surface viscosities in insoluble fatty acid monolayers: Effect of phase transitions on dilational viscoelasticity, Phys. Rev. E **60**, 7163 (1999).
[8] P. He, K. Fang, G. Zou, J. Peltonen, and J. Rosenholm, Elasticity of Langmuir monolayer detected by dynamic oscillation method, Colloids and Surfaces A **201**, 265 (2002).
[9] J. M. Lopez, M. J. Vogel, and A. H. Hirsa, Influence of coexisting phases on the surface dilatational viscosity of Langmuir monolayers, Phys. Rev. E **70**, 056308 (2004).
[10] V. E. Cuenca, M. Fernández Leyes, R. D. Falcone, N. M. Correa, D. Langevin, and H. Ritacco, Interfacial dynamics and its relations with "negative" surface viscosities measured at water–air interfaces covered with a cationic surfactant, Langmuir **35**, 8333 (2019).
[11] A. Shmyrov and A. Mizev, Surface diffusion in gaseous monolayers of an insoluble surfactant, Langmuir **35**, 14180 (2019).
[12] C. Maldarelli, Respiratory distress when a lung surfactant loses one of its two hydrophobic tails, Proc. Nat. Acad. Sci. USA **121**, e2320426121 (2024).
[13] L. E. Scriven, Dynamics of a fluid interface equation of motion for Newtonian surface fluids, Chem. Eng. Sci. **12**, 98 (1960).
[14] Experiments were run at five combinations of (δ, ω): $(1.5\,\mathrm{cm}, 7.4\,\mathrm{rad/s})$, $(1.0\,\mathrm{cm}, 7.4\,\mathrm{rad/s})$, $(0.5\,\mathrm{cm}, 7.4\,\mathrm{rad/s})$, $(1.0\,\mathrm{cm}, 3.7\,\mathrm{rad/s})$, and $(1.5\,\mathrm{cm}, 2.5\,\mathrm{rad/s})$.
[15] M. J. Vogel, A. H. Hirsa, and J. M. Lopez, Spatiotemporal dynamics of a periodically driven cavity flow, J. Fluid Mech. **478**, 197–226 (2003).
[16] See Supplemental Material at [URL will be inserted by publisher] for a movie animating the simulated velocity magnitude $\|\boldsymbol{u}\|$ in the channel, together with profiles of surface velocity u^s and monolayer concentration c over one period for $\mathrm{Re} = 600$, $\Omega = 1/3$, $c_0 = 1.5\,\mathrm{mg/m^2}$, $\mathrm{Ca} = 1.645 \times 10^{-3}$, $\mathrm{Sc} = 0.0023$, and $\mathrm{Bq} = 1$.
[17] The advection-diffusion equation for the monolayer concentration c, Eq. (3), is linear in c, and so c is kept dimensional throughout.
[18] H. M. McConnell, Structures and transitions in lipid monolayers at the air-water interface, Ann. Rev. Phys. Chem. **42**, 171 (1991).
[19] The BAM image was obtained under quasi-static compression of a DPPC monolayer in a Langmuir trough and shows co-existent LE+LC domains of size $\sim 10\mu$m.
[20] R. Peters and K. Beck, Translational diffusion in phospholipid monolayers measured by fluorescence microphotolysis., Proc. Nat. Acad. Sci. **80**, 7183 (1983).
[21] L. R. Arriaga, I. López-Montero, J. Ignés-Mullol, and F. Monroy, Domain-growth kinetic origin of nonhorizontal phase coexistence plateaux in Langmuir monolayers: compression rigidity of a raft-like lipid distribution, J. Phys. Chem. B **114**, 4509 (2010).
[22] I. López-Montero, L. R. Arriaga, F. Monroy, G. Rivas, P. Tarazona, and M. Vélez, High fluidity and soft elasticity of the inner membrane of escherichia coli revealed by the surface rheology of model Langmuir monolayers, Langmuir **24**, 4065 (2008).
[23] H. Maru and D. Wasan, Dilational viscoelastic properties of fluid interfaces II: experimental study, Chem. Eng. Sci.

34, 1295 (1979).

[24] F. Monroy, M. G. Munoz, J. E. F. Rubio, F. Ortega, and R. G. Rubio, Capillary waves in ionic surfactant solutions: effects of the electrostatic adsorption barrier and analysis in terms of a new dispersion equation, J. Phys. Chem. B **106**, 5636 (2002).

[25] G. L. Gaines, *Insoluble Monolayers at Liquid-gas Interfaces* (Wiley-Interscience, 1966).

[26] L. Arriaga, I. Lopez-Montero, R. Rodríguez-García, and F. Monroy, Nonlinear dilational mechanics of Langmuir lipid monolayers: A lateral diffusion mechanism, Phys. Rev. E **77**, 061918 (2008).